BİTLİS EREN ÜNİVERSİTESİ
FEN BİLİMLERİ DERGİSİ

ISSN: 2147-3129 / e-ISSN: 2147-3188

Article Type : Research Article
Received : January 28, 2025
Revised : March 13, 2025
Accepted : March 17, 2025
DOI : 10.17798/bitlisfen.1628206

Year : 2025
Volume : 14
Issue : 1
Pages : 633-646

CAFFEINE COATED IRON OXIDE CRUSTACEAN FOR AMMONIA BORANE DEHYDROGENATION DEVELOPMENT OF MAGNETIC NICKEL NANOPARTICLES

Erhan ONAT [1]

[1] *Bitlis Eren University, Department of Electricity and Energy, Bitlis, Türkiye, eonat@beu.edu.tr*

ABSTRACT

The aim of this study was to develop nickel (Ni) nanoclusters with caffeine-coated magnetic iron oxide (Fe_3O_4) center shells for the catalytic hydrolysis of ammonia borane (AB). In the study, magnetic iron oxide (MIO) clusters were obtained by hydrothermal treatment. These clusters were first coated with caffeine according to the reflux method at 150 °C for 12 hours, and then Ni was decorated on these clusters by impregnation method. Magnetic Ni catalyst ($Ni@C/Fe_3O_4$) was synthesized by dropping 10 M 20 mL sodium borohydride ($NaBH_4$-SBH) into the Ni-C/ Fe_3O_4 magnetic nanoclusters in solution as a result of the loading processes carried out at room conditions. After filtration, washing and drying in nitrogen atmosphere, the crumbled catalyst was identified by advanced identification techniques (FT-IR, BET, SEM, EDX, XPS) and used in AB hydrolysis.

The solvate medium, catalyst amount, AB concentration, temperature and repeated use parameters were investigated for AB catalytic hydrolysis. As a result of the optimization at 303 K, the best hydrogen production was determined as 7873 mL/g.min using 2.5 % NaOH, 30 mg catalyst and 300 mM AB. The catalyst cycle frequency (TOF) was measured as 1447 s^{-1}. As a result of reaction kinetics investigations, it was determined that the reaction was 1st order and the reaction activation energy was 35.07 kJ/mol.

Keywords: Ammonia borane, Dehydrogenation, Fe_3O_4, Hydrolysis, Catalyst, $Ni@C/Fe_3O_4$.

1 INTRODUCTION

Renewable energy sources are the solution to reduce the negative impact of greenhouse gases caused by fossil fuels on the world. When alternative energy sources are examined in general, it will be seen that solar energy, wind energy, biomass energy, tidal energy, geothermal

energy and hydrogen energy are used as alternative energy sources. These alternative energy sources are preferred at different levels according to country conditions. Renewable energy source technology is currently being used and continues its development in parallel with the studies carried out by researchers. Hydrogen energy technology, which enables energy production at different values at regional and seasonal levels due to its various limitations, is an energy technology with many advantages [1] – [3].

Hydrogen is one of the best alternative energy carriers to meet the demand for efficient and clean energy in terms of being obtained from many sources, high energy density and not having a harmful effect on the environment [4].

Hydrogen is a colorless, odorless gas that makes up 75% of the mass of the universe. Hydrogen, which is converted into energy in fuel units, is expected to be used as fuel in vehicles and airplanes in the near future. Hydrogen is a non-toxic, inexhaustible and renewable source of clean energy. Hydrogen is a gas that can be stored, transported, converted into other forms of energy, and energy can be obtained with high efficiency. An important feature of hydrogen is that it cannot be used as a primary energy source. Hydrogen is converted into energy in fuel cells [5], [6].

Hydrogen converted into energy in fuel cells is currently used as a gas. Since hydrogen is a gas that takes up a lot of volume, storing and transporting it as a gas causes safety risks and cost losses. This problem is largely overcome by storing hydrogen in different ways. The most important storage technique is the solid storage of hydrogen in boron-based compounds. When the compounds used in hydrogen storage are examined, it is seen that ammonia borane takes the lead. Ammonia borane offers many advantages such as high hydrogen storage (19.6% by mass), stability up to high temperatures, non-toxicity, and the possibility of hydrogen production from water in addition to hydrogen in its own structure as a result of hydrolysis [7] – [9].

As with other compounds in which hydrogen is chemically stored, hydrogen production (dehydrogenation) from ammonia borane is realized by catalytic reactions under catalyst control. The hydrolysis reaction for the catalytic reaction of ammonia borane is given in Equation 1.

$$NH_3BH_3 + 2H_2O \rightarrow NH_4BO_2 + 3H_2 \quad (1)$$

The fact that the reaction is catalyst-controlled and makes it possible to produce hydrogen from water makes the use of ammonia borane as a hydrogen storage source more important [10], [11].

The re-release of hydrogen from boron compounds is realized by catalytic processes using catalysts. Catalysts are generally defined as substances that increase the reaction rate. Catalysts, which are not among the substances that react or are formed, are involved in increasing the reaction rate by reducing the activation energy of the reaction. In systems where catalysts are used, energy loss is prevented and time is saved. Catalyst structures are highly preferred thanks to their advantages such as ensuring product control in the catalytic process, preventing loss of time, and reducing energy costs to low levels [12] – [14]

Features such as repeated use of catalysts, recovery and production from environmentally friendly materials make the material from which the catalyst is developed important. These properties are largely present in magnetic nanoparticles. Magnetic nanoparticles are a type of particle with a very wide range of applications. Therefore, there are many production methods. Depending on technological developments, magnetic nanoparticle production continues its development [15] – [17].

Today, magnetic nanoparticle production methods are co-precipitation, microemulsion, thermal decomposition, solvothermal (hydrothermal) synthesis, chemical reduction, sonochemical reactions, microwave method, chemical vapor deposition, arc discharge, laser pyrolysis, combustion synthesis, annealing methods [18].

Magnetic material is used in many fields such as superparamagnetism, high sensitivity, biocompatibility, separation technology, protein immobilization, catalysis, adsorption, drug/gene delivery, biosensors, magnetic resonance imaging, contrast enhancement, biophotonics, detection of cancer cells and tissue engineering. Among these areas of use, adsorption and catalytic processes are the most widely used areas of magnetic nanoparticles [19] – [23].

In this study, environmentally friendly magnetic nanoparticles were synthesized by hydrotemal method and the synthesized nanoparticles were used as support material for the catalyst structure obtained from nickel metal. In the presence of synthesized nickel-based magnetic nanoparticle catalyst structures, the parameters of hydrogen production (dehydrogenation) by hydrolysis from ammonia borane were investigated.

2 MATERIAL AND METHOD

Among the chemicals used in the study; Ammonia borane (AB), Sodium borhydride (SBH-$NaBH_4$) Sodium hydroxide (NaOH), Nickelchloride hexahydrate ($NiCl_2{\times}6H_2O$), Iron (II) chloride tetrahydrate ($FeCl_2{\times}4H_2O$), Iron (III) chloride hexahydrate ($FeCl_3{\times}6H_2O$) were obtained from Sigma Aldrich and ammonia (NH_3) was obtained from TEKKİM. Ultrapure water was used in synthesis and hydrolysis processes. The devices used in the study were an oven, magnetic stirrer with heater, precision balance and gas collection unit. The oven was used in drying processes, the magnetic stirrer in reduction and metal loading processes, the precision balance in weighing processes, and the gas collection unit in time-dependent hydrogen production processes.

In the study, MIO was produced by hydrothermal method according to Equation 2 by taking the amount of material. In this process, metal salts containing Fe^{2+} and Fe^{3+} ions were taken into autoclave with pure water (50 mL of pure water and 10 mL of ammonia) by adding ammonia so that the pH was around 11.

$$Fe^{2+} + Fe^{3+} + 8\ OH^- \rightarrow Fe_3O_4 + 4\ H_2O \quad (2)$$

The autoclave was kept at 180 °C for 8 hours and then the autoclave was allowed to come to room temperature. The obtained MIO was magnetically washed 7-8 times and Fe_3O_4 was obtained by vacuum filtration. Then, the magnetic material was allowed to dry at 60 °C for 16 hours in nitrogen atmosphere. The dried MIO and caffeine were taken in a 1:1 ratio and refluxed in distilled water at 150 °C for 12 hours. Then, after magnetic washing and drying in nitrogen atmosphere, nickel plating of the magnetic material to be used as support material was performed by impregnation method. For this process, Ni salt dissolved in pure water was dripped at 750 rpm under room conditions on the support material, which was also well dispersed in pure water. After 2-3 hours of dripping, the sample was stirred in a magnetic stirrer in pure water for 24 hours under room conditions. After Ni decoration, 10 M 20 mL SBH solution was dripped onto the mixture to reduce Ni metal atoms on the support surface. After the dropping process, the mixture was kept for about 2 hours and it was observed that the bubbles stopped coming out. Then, the catalyst separated from the filtrate by vacuum filtration was kept at 70 °C in the presence of nitrogen gas for 12 hours to dry [24] – [26]. The dried magnetic material coated caffeine nickel catalyst (Ni@C/Fe_3O_4) was crumbled and its structure was investigated. FT-IR, BET, SEM, EDX, XPS, SEM, EDX and XPS analyses were performed to elucidate the material structure. After structure elucidation, AB catalytic hydrolysis reactions

were carried out. Hydrolysis reactions were interpreted according to the formation of H_2 amount. For this process, water-gas displacement was utilized and the amount of H_2 released over time was recorded with the help of a stopwatch. The best hydrogen production values were determined as a result of parameter investigations such as support loading, solution medium and catalyst amount.

3 RESULTS AND DISCUSSION

The magnetic properties of the materials synthesized within the scope of the study were tested in solution and solid media. Images of these test processes are given in Figure 1.

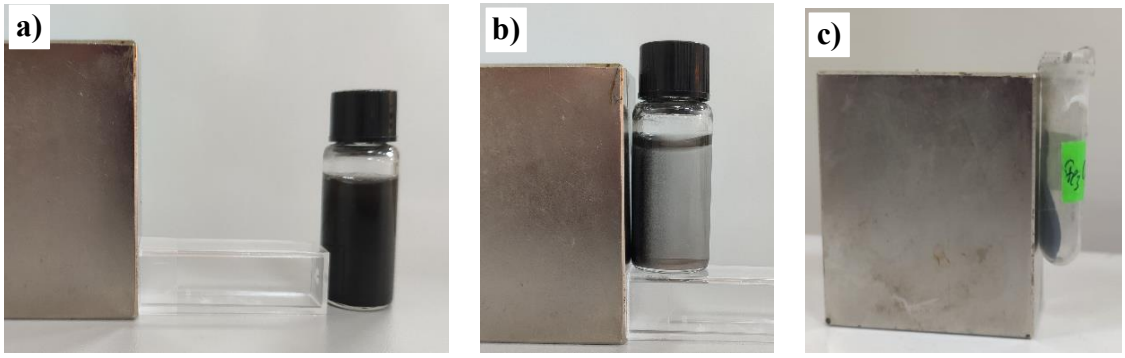

Figure 1. Behavior of magnetic Ni@C/Fe$_3$O$_4$ in magnetic field (a) Before magnetic field (b) In water in magnetic field (c) In solid state in magnetic field.

3.1 Characterization of Fe$_3$O$_4$ and Ni@C/Fe$_3$O$_4$

FT-IR, EDX, SEM and BET analyses were performed to characterize the structure of the samples that were found to have magnetic properties. When FT-IR given in Figure 2 is analyzed, it is seen that there is no significant shift in the outlines. This means that the coated material does not disturb the magnetic structure. When only the peaks of Fe_3O_4 are analyzed, it is seen that the prominent Fe_3O_4 peaks between 980-1200 cm^{-1} disappear completely after caffeine and Ni coating. This means that the coating and decoration were successfully realized. The caffeine-induced C-C and C-N peaks in the 800-950 cm^{-1} range also confirm this data [27] – [29].

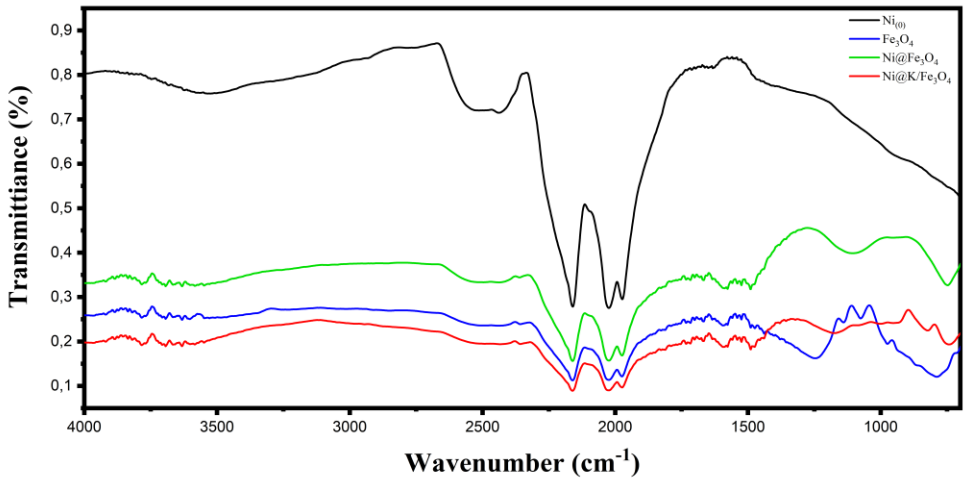

Figure 2. FT-IR image of $Ni_{(0)}$, Fe_3O_4, $Ni@Fe_3O_4$, $Ni@C/Fe_3O_4$ synthesized in this study.

EDX data given in Figures 3 and 4 confirm that Fe_3O_4 and $Ni@C/Fe_3O_4$ were successfully synthesized within the scope of the study. SEM analysis of the material consisting only of Fe_3O_4 magnetic material is given in Figure 3. In the figure, it is seen that a magnetic material in the form of a ball rod with a weight in the form of a rod is obtained. It is understood from the SEM images that the average particle diameter of the material in question is 51 nm. SEM analysis of $Ni@C/Fe_3O_4$ magnetic nanoparticles obtained after loading Fe_3O_4 with caffeine and Ni is given in Figure 4. As seen in the figure, it is seen that the particles, which are predominantly rod-shaped as a result of caffeine and Ni loading, have a spherical structure. It is understood from Figure 4 that $Ni@C/Fe_3O_4$ magnetic nanoparticles with a diameter of 24.6 nm instead of the average 51 nm formed only by magnetic iron oxides. BET analysis also confirms this situation. Because while Fe_3O_4 BET surface analysis is 13.7167 m^2/g, $Ni@C/Fe_3O_4$ BET surface analysis is 47.5764 m^2/g. This means that the effective catalytic surface is more [30].

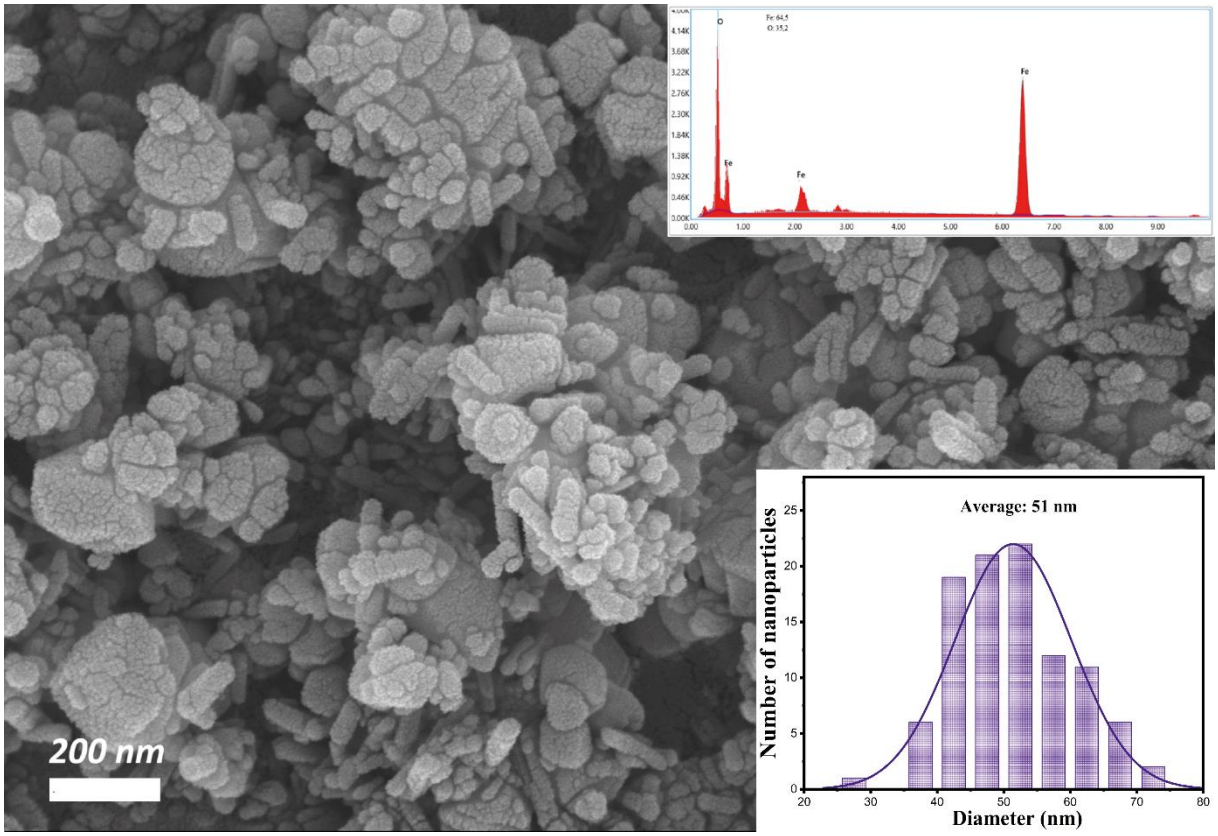

Figure 3. SEM, EDX analysis and average particle diameters of Fe_3O_4.

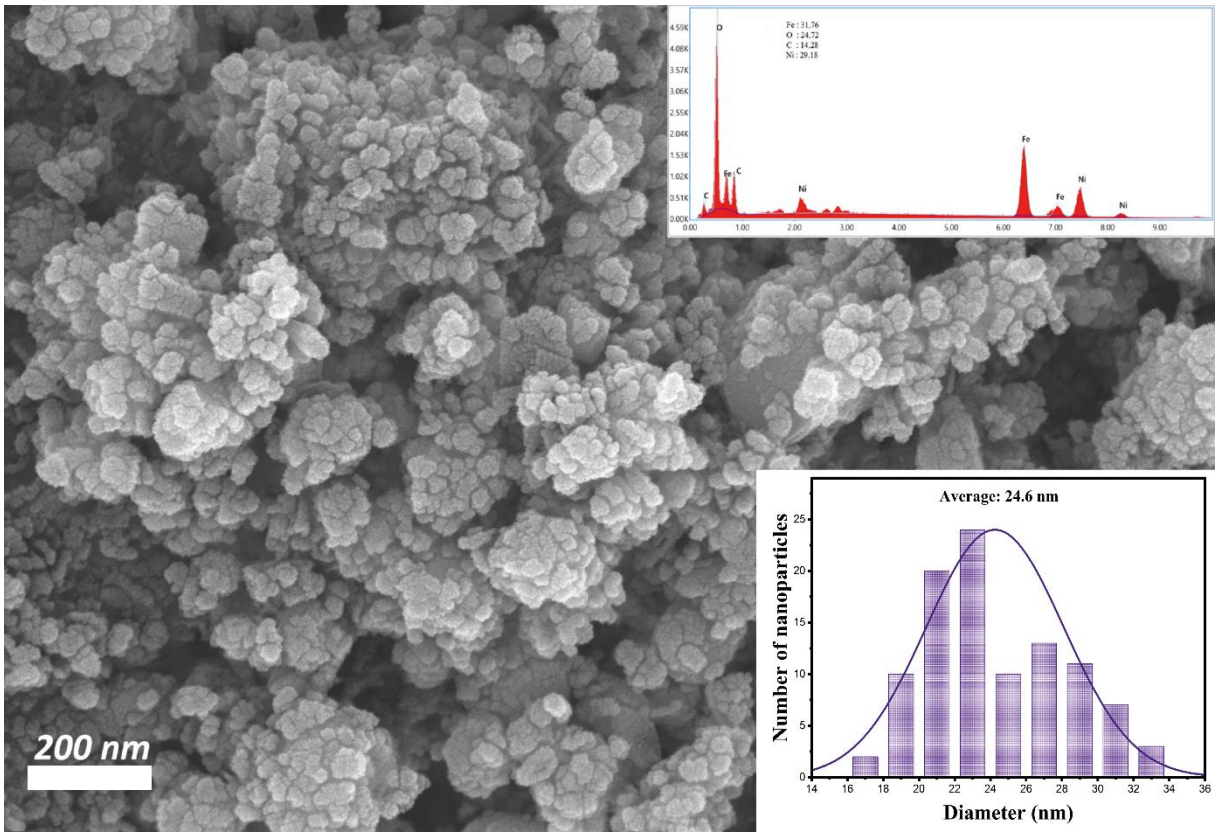

Figure 4. SEM, EDX analysis and average particle diameters of Ni@C/Fe_3O_4.

XPS analyses performed to determine the behavior of the electrons in the Ni metal atom clusters successfully attached to the Fe_3O_4@C surface as a result of reduction under SBH are given in Figure 5. In the XPS analysis of magnetic Ni nanoparticles, which were determined to have a high catalytic effect within the scope of the study, significant peaks of 858 eV for $Nip_{3/2}$, 864 eV for $Nis_{1/2}$ and 533 eV for O1s were detected [26], [31]. These XPS analyzes are given in Figure 5.

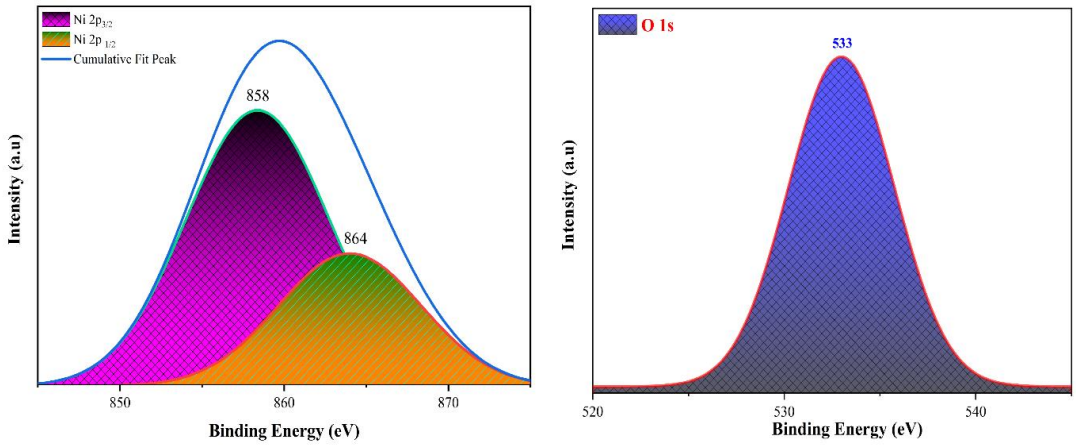

Figure 5. XPS analysis of Ni@C/Fe_3O_4.

3.2 Dehydrogenation

After the determination of the material structure, the dehydrogenation parameter investigation of the study was carried out. These processes are given respectively. First of all, the parameters of $Ni_{(0)}$ for nickel loading, nickel loading on magnetic material and caffeine and then nickel loading on magnetic material were investigated. As a result of the hydrolysis process for three different structures, the degradation values of ammonia borane over time due to hydrogen formation are shown in Figure 6 a. It is clearly seen that the caffeine coated magnetic material shows high catalytic effect. After the determination of the support loading pattern, it is understood from Figure 6 b that the best H_2 production from hydrolysis reactions carried out at different NaOH concentrations is at 2.5 % NaOH. It is evaluated that hydrogen yield decreases at concentrations above 2.5% because metaborate screens the catalyst surface. As a result of the catalytic hydrolysis reactions carried out with different catalyst amounts in the continuation of the study, it is seen in Figure 6 c that the reaction time shortens with increasing catalyst amount. In the calculations for the best H_2 production per catalyst, it was determined that the highest H_2 yield was 4978 mL/g.min at 30 mg catalyst. This can be attributed to the best combination concentration of catalyst and hydrogen source. Hydrolysis data obtained as a result

of dehydrogenation processes carried out at different AB concentrations are given in Figure 6 d. As seen in the figure, H_2 production increases with increasing AB concentration. 7873 mL/g.min H_2 yield was obtained as a result of catalytic dehydrogenation with 300 mM AB. This value is quite high for Ni metal AB dehydrogenation [10].

As a result of optimization procedures with Ni@C/Fe_3O_4 for H_2 production, 2.5 % NaOH, 30 mg catalyst usage and 300 mM AB concentration were determined for the best hydrolysis data at 303 K. H_2 production at these values is 7873 mL/g.min per catalyst amount.

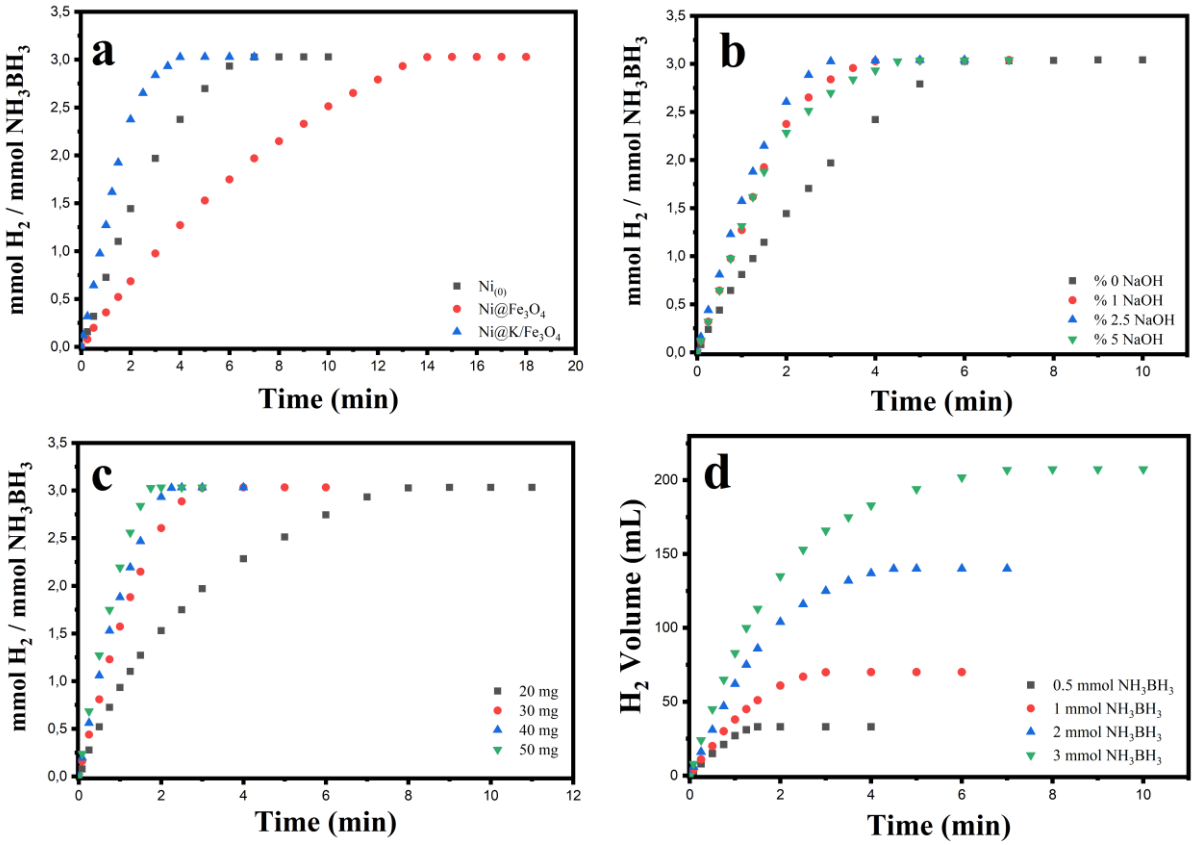

Figure 6. Ni@C/Fe_3O_4 catalytic dehydrogenation data; a) support loading, b) NaOH effect, c) catalyst amount, d) AB concentration.

After the completion of H_2 optimization, hydrolysis reactions at different temperatures were carried out for the kinetic data analysis of equation 1 catalyzed by Ni@C/Fe_3O_4 catalyst. The data for these reactions are given in Figure 7 a. As seen in the figure, the reaction accelerates in parallel with increasing temperature. As a result of the 0th, 1st and nth reaction equation correlations of the catalytic hydrolysis data performed at 30, 40, 50 and 60 °C, it was determined that the AB hydrolysis reaction catalyzed by Ni@C/Fe_3O_4 catalyst was 1st order. Based on the 1st order reaction data, when the graph of ln k versus 1/T is plotted, we see a graph as shown

in Figure 7 b. When the relevant data were substituted in the Arrhenius equation (Equation 3), the activation energy (Ea) of the reaction was determined as 35.07 kJ/mol [32].

$$lnk = lnA\text{-}Ea \,/\, RT \tag{3}$$

Six consecutive hydrolysis reactions were carried out for repeated use of the catalyst. After each use, 90% of the solution was decanted into a different container and a new hydrogen source was added and 100% product yield was achieved in all repeated uses (Figure 7 c). The slight decrease in catalytic activity due to repeated use can be attributed to the deformation of the catalyst active surface. It is considered that the main factor in this deformation is due to the adhesion of sodium hydroxide and metaborate to the catalyst surface [33], [34].

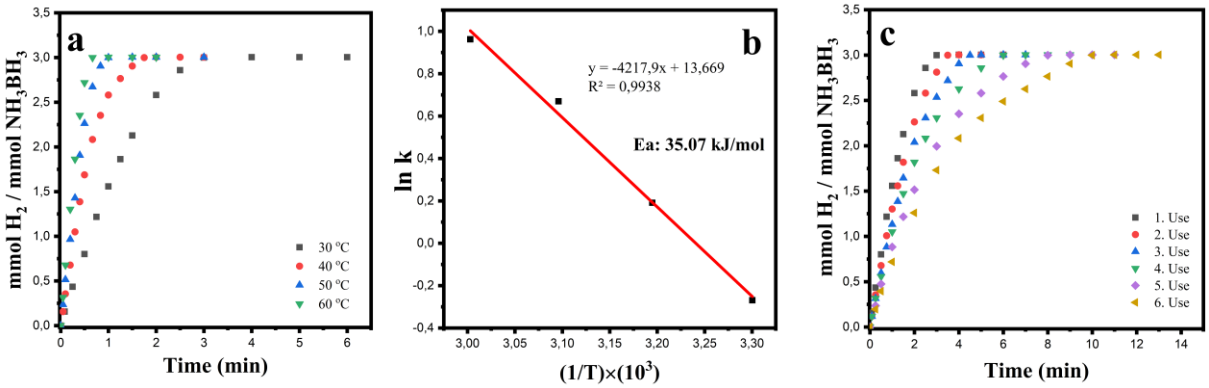

Figure 7. Ni@C/Fe₃O₄ catalytic dehydrogenation data; a) Temperature effect, b) Arrhenius equation data, c) Catalyst repeated use.

Another key parameter measured to determine catalyst efficiency is the catalytic efficiency cycle frequency (TOF) value. Hydrogen is formed as a product at the end of ammonia borane decomposition. In this study, the cycle frequency was measured in terms of the number of moles of hydrogen (product) formed depending on the number of moles of magnetic nickel catalyst according to the following equation (Equation 4).

$$\text{TOF} = \frac{Mole\ Amount\ of\ the\ Product}{Mole\ Amount\ of\ catalystı\ \times\ Time} \tag{4}$$

The TOF value was determined as 1447 s^{-1} in the calculations made at the highest value measured for hydrogen velocity within the scope of the study.

4 CONCLUSION AND SUGGESTIONS

Within the scope of the study, magnetic material synthesis was successfully realized by hydrothermal method. As a result of the analysis for structure identification, it was determined that the magnetic nanomaterial was synthesized as targeted at the beginning of the study. It was understood from the decomposition data of the ammonia borane reaction that the catalytic effect of the synthesized magnetic nickel nanoparticles was high. When the studies in which nickel metal catalyzed the decomposition of ammonia borane as a catalyst were examined (Table 1), it was understood that the catalyst structure was synthesized at low activation energy and high hydrogen production rate.

Table 1. Some studies in which ammonia borane was catalyzed in the presence of nickel catalyst.

Catalyst	Ea ($k.J.mol^{-1}$)	HGR (mL/g.min)	TOF (s^{-1})	Temperature (^{o} C)	Reference
Ni/C	31.6	834	-	25	[35]
Pt_x-Ni-$_{1-x}$	39	4784.7	-	30	[36]
Pt-Ni	46.8	1299.2	751	25	[37]
$Ni_{0.33}$@$Pt_{0.67}$/C	33	5469	-	30	[38]
Ni/SiO_2	34	-	132	25	[39]
Ni@C/Fe_3O_4	35.07	7873	1447	30	**This study**

In this study in which ammonia borane degradation data were investigated in the presence of magnetic nickel nanoparticles; it was determined that 2.5 % NaOH was used as the best solvent medium, 30 mg of catalyst was used as the best catalyst amount and hydrogen production rate increased in parallel with increasing ammonia borane concentration. It was determined that 7873 mL/g.min hydrogen production rate was achieved as a result of catalytic decomposition with 300 nM ammonia borane at 30 ^{o}C under the best conditions. The catalytic activity cycle frequency (TOF) at the best hydrogen production rate was measured as 1447 s^{-1}. As a result of the analysis and calculations for the reaction kinetics of the catalytic process, it was determined that the reaction was 1st order. The activation energy (Ea) of the reaction was determined as 35.07 kJ/mol. This shows that Ni@C/Fe_3O_4 catalyst reduces the reaction activation energy to very low values. It is evaluated that both the magnetic nanoparticle to be used in hydrogen production and other catalytic processes, decorating the magnetic material with active metal after caffeine coating will create a high catalytic effect.

Statement of Research and Publication Ethics

The study is complied with research and publication ethics.

Artificial Intelligence (AI) Contribution Statement

This manuscript was entirely written, edited, analyzed, and prepared without the assistance of any artificial intelligence (AI) tools. All content, including text, data analysis, and figures, was solely generated by the author.

REFERENCES

[1] P. J. Megía, A. J. Vizcaíno, J. A. Calles, and A. Carrero, "Hydrogen production technologies: From fossil fuels toward renewable sources. A mini review," *Energy Fuels*, vol. 35, no. 20, pp. 16403–16415, 2021.

[2] A. Pareek, R. Dom, J. Gupta, J. Chandran, V. Adepu, and P. H. Borse, "Insights into renewable hydrogen energy: Recent advances and prospects," *Mater. Sci. Energy Technol.*, vol. 3, pp. 319–327, 2020.

[3] E. Onat, F. A. Celik, E. Karabulut, and M. S. Izgi, "High availability and outstanding catalytic activity in sodium borohydride hydrolytic dehydrogenation of CQD/GO@Co catalyst by green synthesis: Experimental and computational perspective," *Int. J. Hydrogen Energy*, vol. 83, pp. 903–915, 2024.

[4] A. Midilli and I. Dincer, "Hydrogen as a renewable and sustainable solution in reducing global fossil fuel consumption," *Int. J. Hydrogen Energy*, vol. 33, no. 16, pp. 4209–4222, 2008.

[5] M. A. Rosen and S. Koohi-Fayegh, "The prospects for hydrogen as an energy carrier: an overview of hydrogen energy and hydrogen energy systems," *Energy Ecol. Environ.*, vol. 1, no. 1, pp. 10–29, 2016.

[6] E. L. V. Eriksson and E. M. Gray, "Optimization and integration of hybrid renewable energy hydrogen fuel cell energy systems—A critical review," *Appl. Energy*, vol. 202, pp. 348–364, 2017.

[7] W. Jiao et al., "Magnetic Ni and Ni/Pt hollow nanospheres and their catalytic activities for hydrolysis of ammonia borane," *J. Mater. Chem. A Mater. Energy Sustain.*, vol. 2, no. 43, pp. 18171–18176, 2014.

[8] E. Onat, F. A. Çelik, Ö. Şahin, E. Karabulut, and M. S. İzgi, "H2 production from ammonia borane hydrolysis with catalyst effect of titriplex® III carbon quantum dots supported by ruthenium under different reactant conditions: Experimental study and predictions with molecular modelling," *Int. J. Hydrogen Energy*, 2024.

[9] U. B. Demirci, "Ammonia borane, a material with exceptional properties for chemical hydrogen storage," *Int. J. Hydrogen Energy*, vol. 42, no. 15, pp. 9978–10013, 2017.

[10] W.-W. Zhan, Q.-L. Zhu, and Q. Xu, "Dehydrogenation of ammonia borane by metal nanoparticle catalysts," *ACS Catal.*, vol. 6, no. 10, pp. 6892–6905, 2016.

[11] R. P. Shrestha, H. V. K. Diyabalanage, T. A. Semelsberger, K. C. Ott, and A. K. Burrell, "Catalytic dehydrogenation of ammonia borane in non-aqueous medium," *Int. J. Hydrogen Energy*, vol. 34, no. 6, pp. 2616–2621, 2009.

[12] A. K. Figen, "Dehydrogenation characteristics of ammonia borane via boron-based catalysts (Co–B, Ni–B, Cu–B) under different hydrolysis conditions," *Int. J. Hydrogen Energy*, vol. 38, no. 22, pp. 9186–9197, 2013.

[13] M. S. İzgi, Ö. Şahin, E. Onat, and S. Horoz, "Metanolde sentezlenen Co-B katalizörün sodyum hidrolizi üzerine etkisi," *J. Inst. Sci. Technol.*, vol. 7, no. 4, pp. 151–160, 2017.

[14] N. C. Smythe and J. C. Gordon, "Ammonia borane as a hydrogen carrier: Dehydrogenation and regeneration," *Eur. J. Inorg. Chem.*, vol. 2010, no. 4, pp. 509–521, 2010.

[15] H. Cui, Y. Liu, and W. Ren, "Structure switch between α-Fe_2O_3, γ-Fe_2O_3 and Fe_3O_4 during the large scale and low temperature sol–gel synthesis of nearly monodispersed iron oxide nanoparticles," *Adv. Powder Technol.*, vol. 24, no. 1, pp. 93–97, 2013.

[16] M. Seehra, *Magnetic Spinels: Synthesis, Properties and Applications*, Bod–Books on Demand, 2017.

[17] M. S. İzgi, M. Ş. Ece, H. Ç. Kazici, Ö. Şahin, and E. Onat, "Hydrogen production by using Ru nanoparticle decorated with Fe_3O_4@SiO_2-NH_2 core-shell microspheres," *Int. J. Hydrogen Energy*, vol. 45, no. 55, pp. 30415–30430, 2020.

[18] Y. Hao and A. S. Teja, "Continuous hydrothermal crystallization of α–Fe_2O_3 and Co_3O_4 nanoparticles," *J. Mater. Res.*, vol. 18, no. 2, pp. 415–422, 2003.

[19] S. Gil, C. R. Correia, and J. F. Mano, "Magnetically labeled cells with surface-modified Fe_3O_4 spherical and rod-shaped magnetic nanoparticles for tissue engineering applications," *Adv. Healthcare Mater.*, vol. 4, no. 6, pp. 883–891, 2015.

[20] S. Shabestari Khiabani, M. Farshbaf, A. Akbarzadeh, and S. Davaran, "Magnetic nanoparticles: preparation methods, applications in cancer diagnosis and cancer therapy," *Artif. Cells Nanomed. Biotechnol.*, vol. 45, no. 1, pp. 6–17, 2017.

[21] D. V. Voronin et al., "In vitro and in vivo visualization and trapping of fluorescent magnetic microcapsules in a bloodstream," *ACS Appl. Mater. Interfaces*, vol. 9, no. 8, pp. 6885–6893, 2017.

[22] L. Xu, M.-J. Kim, K.-D. Kim, Y.-H. Choa, and H.-T. Kim, "Surface modified Fe_3O_4 nanoparticles as a protein delivery vehicle," *Colloids Surf. A Physicochem. Eng. Asp.*, vol. 350, no. 1–3, pp. 8–12, 2009.

[23] S. Liu, H. Chen, X. Lu, C. Deng, X. Zhang, and P. Yang, "Facile synthesis of copper (II) immobilized on magnetic mesoporous silica microspheres for selective enrichment of peptides for mass spectrometry analysis," *Angew. Chem. Int. Ed.*, vol. 41, no. 49, pp. 7557–7561, 2010.

[24] E. Onat, "Synthesis of a cobalt catalyst supported by graphene oxide modified perlite and its application on the hydrolysis of sodium borohydride," *Synth. Met.*, vol. 306, 2024.

[25] E. Onat and S. Ekinci, "A new material fabricated by the combination of natural mineral perlite and graphene oxide: Synthesis, characterization, and methylene blue removal," *Diam. Relat. Mater.*, vol. 143, 110848, 2024.

[26] Ö. Şahin, S. Ekinci, M. S. İzgi, and E. Onat, "Effect of different solvents on hydrogen production from hydrolysis of potassium borohydride with a new and active Ni-based catalyst synthesized by green synthesis," *Int. J. Hydrogen Energy*, 2024.

[27] P. Panneerselvam, N. Morad, and K. A. Tan, "Magnetic nanoparticle (Fe_3O_4) impregnated onto tea waste for the removal of nickel (II) from aqueous solution," *J. Hazard. Mater.*, vol. 186, no. 1, pp. 160–168, 2011.

[28] A. Mulyasuryani, R. Tjahjanto, and R. Andawiyah, "Simultaneous voltammetric detection of acetaminophen and caffeine base on cassava starch–Fe_3O_4 nanoparticles modified glassy carbon electrode," *Chemosensors*, vol. 7, no. 4, p. 49, 2019.

[29] H. İ. Ulusoy, E. Yılmaz, and M. Soylak, "Magnetic solid phase extraction of trace paracetamol and caffeine in synthetic urine and wastewater samples by a using core-shell hybrid material consisting of graphene oxide/multiwalled carbon nanotube/Fe_3O_4/SiO_2," *Microchem. J.*, vol. 145, pp. 843–851, 2019.

[30] H. W. Di, Y. L. Luo, F. Xu, Y. S. Chen, and Y. F. Nan, "Fabrication and caffeine release from Fe_3O_4/P(MAA-co-NVP) magnetic microspheres with controllable core-shell architecture," *J. Biomater. Sci.*, vol. 22, no. 4–6, pp. 557–576, 2011.

[31] E. Onat, M. S. İzgi, Ö. Şahin, and C. Saka, "Nickel/nickel oxide nanocomposite particles dispersed on carbon quantum dot from caffeine for hydrogen release by sodium borohydride hydrolysis: Performance and mechanism," *Diam. Relat. Mater.*, 2024.

[32] E. Onat and S. Ekinci, "Study of the sodium borohydride hydrolysis reaction's performance via a kaolin-supported Co–Cr bimetallic catalyst," *Afyon Kocatepe Univ. J. Sci. Eng.*, vol. 24, pp. 1061–1070, 2024.

[33] S. Ekinci and E. Onat, "Activated carbon assisted cobalt catalyst for hydrogen production: Synthesis and characterization," *Balıkesir Univ. J. Inst. Sci.*, vol. 26, no. 2, pp. 455–471, 2024.

[34] E. Onat, S. Ekinci, Ö. Şahin, and M. S. İzgi, "Effective and environmentally friendly Co nanocatalyst on sodium borohydride hydrolysis in different solvents," *Int. J. Hydrogen Energy*, 2025.

[35] L. Zhou, T. Zhang, Z. Tao, and J. Chen, "Ni nanoparticles supported on carbon as efficient catalysts for the hydrolysis of ammonia borane," Nano Res., vol. 7, no. 5, pp. 774–781, 2014.

[36] X. Yang, F. Cheng, J. Liang, Z. Tao, and J. Chen, "PtxNi$_{1-x}$ nanoparticles as catalysts for hydrogen generation from hydrolysis of ammonia borane," Int. J. Hydrogen Energy, vol. 34, no. 21, pp. 8785–8791, 2009.

[37] J. Zhang, X. Zheng, W. Yu, X. Feng, and Y. Qin, "Unravelling the synergy in platinum-nickel bimetal catalysts designed by atomic layer deposition for efficient hydrolytic dehydrogenation of ammonia borane," Appl. Catal. B, vol. 306, 121116, 2022.

[38] X. Yang, F. Cheng, J. Liang, Z. Tao, and J. Chen, "Carbon-supported Ni$_{1-x}$@Ptx (x = 0.32, 0.43, 0.60, 0.67, and 0.80) core-shell nanoparticles as catalysts for hydrogen generation from hydrolysis of ammonia borane," Int. J. Hydrogen Energy, vol. 36, no. 3, pp. 1984–1990, 2011.

[39] Ö. Metin, S. Özkar, and S. Sun, "Monodisperse nickel nanoparticles supported on SiO_2 as an effective catalyst for the hydrolysis of ammonia–borane," Nano Res., vol. 3, no. 9, pp. 676–684, 2010.